Supplementary Information (SI) for RSC Advances.
This journal is © The Royal Society of Chemistry 2026

Supporting Information

Selenium-Activated Monolithic FeNi Layered Double Hydroxide Electrodes: Binder-Free, Self-Supported Architectures for Durable Alkaline Oxygen Evolution

Alaa Hassan [a,b], Ghada E. Khedr [c], Aya K. Gomaa [a], Laila H. Abdel-Rahman [b], Hussein M. El-Sagher [b], and Nageh K. Allam [a]*

[a]Energy Materials Laboratory (EML), Physics Department, School of Sciences and Engineering, The American University in Cairo, New Cairo 11835, Egypt (*nageh.allam@aucegypt.edu)

[b]Chemistry Department, Faculty of Science, Sohag University, Sohag-82524, Egypt

[c]Department of Analysis and Evaluation, Egyptian Petroleum Research Institute, Cairo, 11727, Egypt

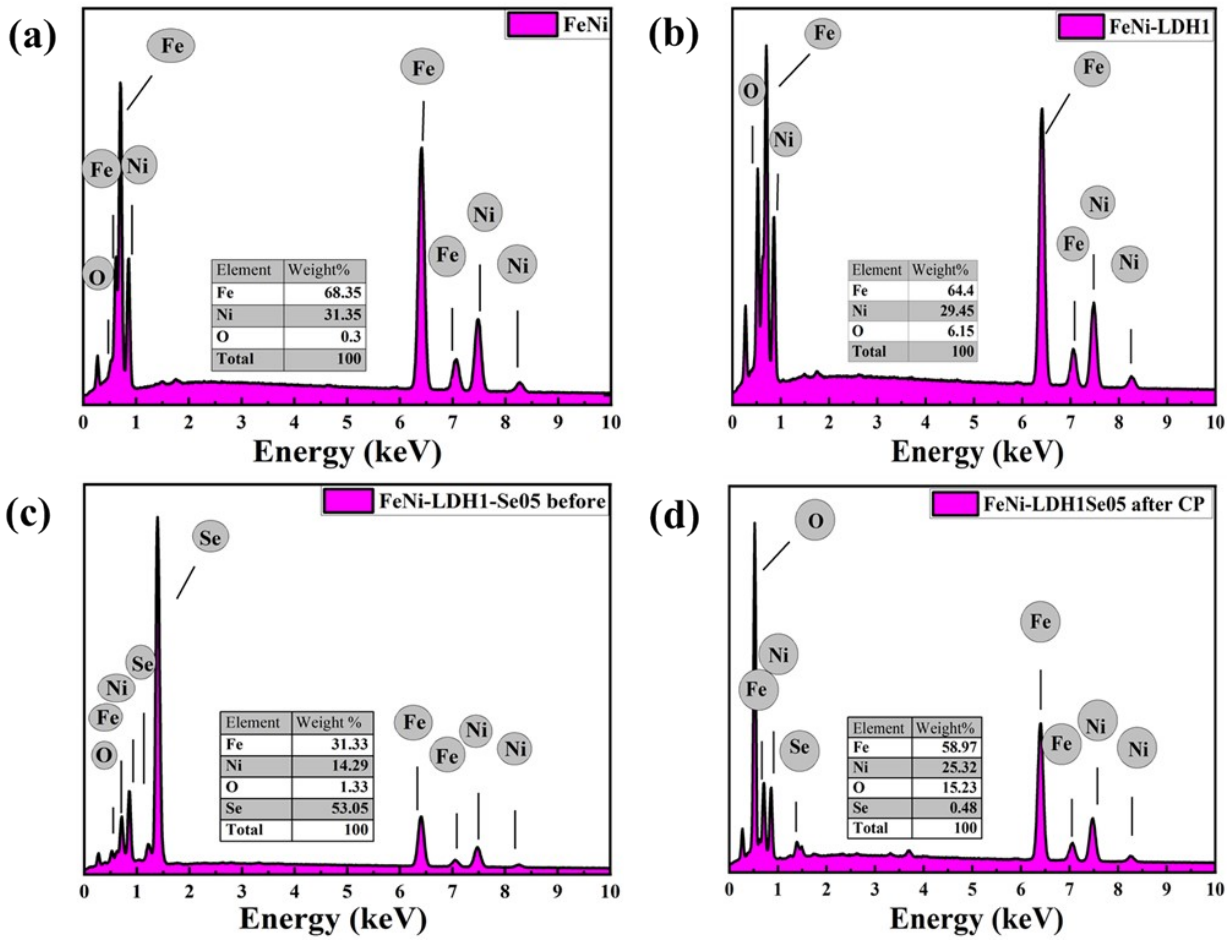

Fig. S1.EDX spectra with elemental weight percentages for the (a) Fe Ni, (b) FeNi-LDH1, (c), and (d) FeNi-LDH1-Se05 catalysts before the OER measurements and after the stability for 5 days @100mA/cm^2, respectively.

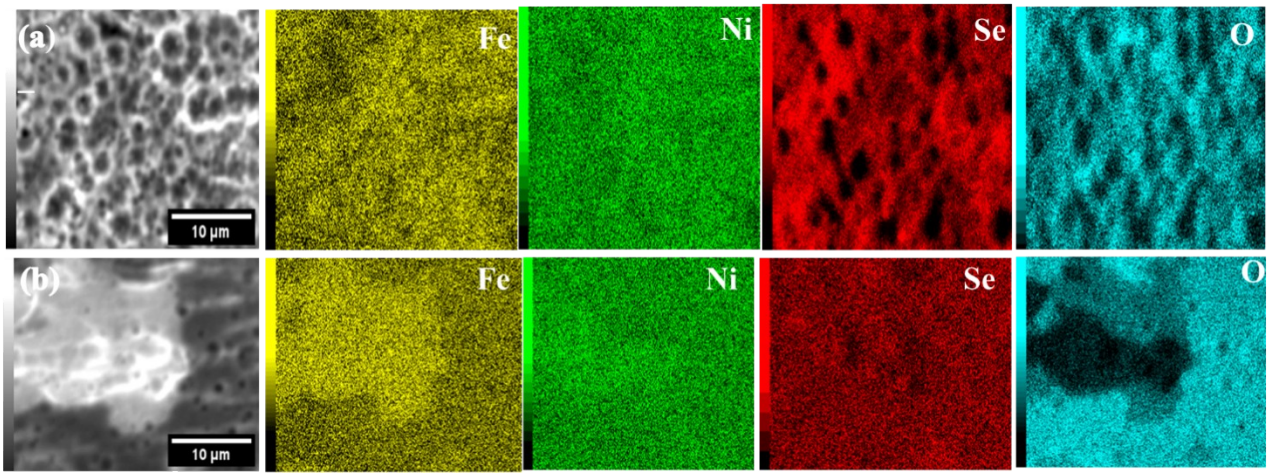

Fig. S2.EDX elemental mapping of the FeNi-LDH1-Se05 catalyst (a) before OER measurements, and (b) after stability @100 mA/cm ^{2} for 5 days.

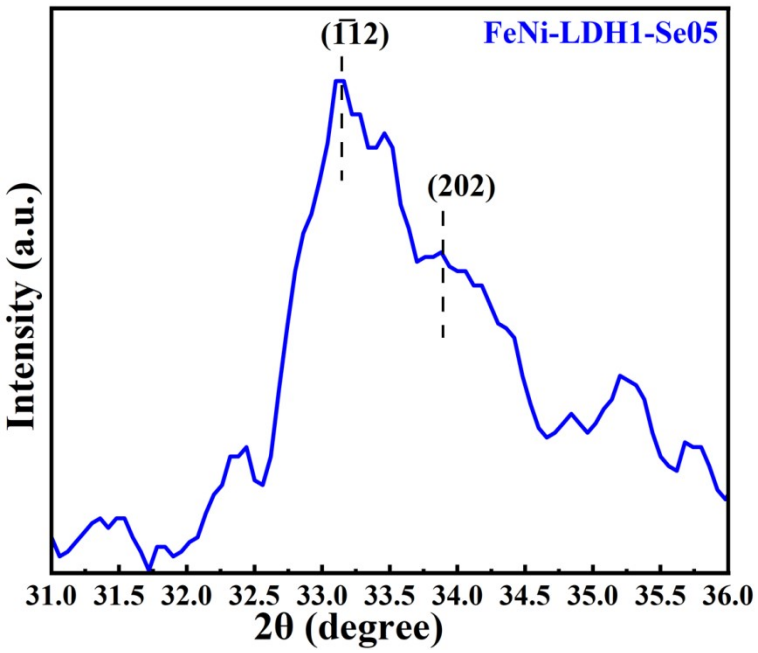

Fig. S3.A magnified XRD spectrum in the range 2θ (31- 36°), displaying two peaks at 33.3 ° and 33.8 °.

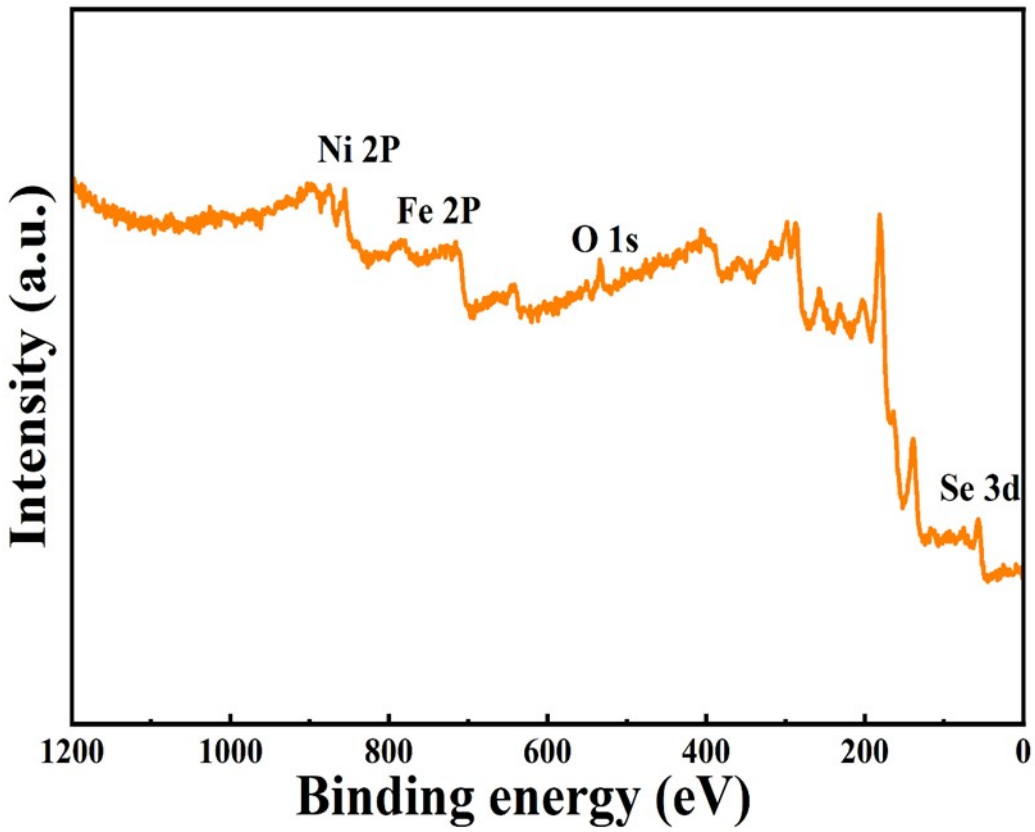

Fig. S4.XPS survey spectrum of the FeNi-LDH1-Se05 catalyst showing Fe, Ni, O, and Se.

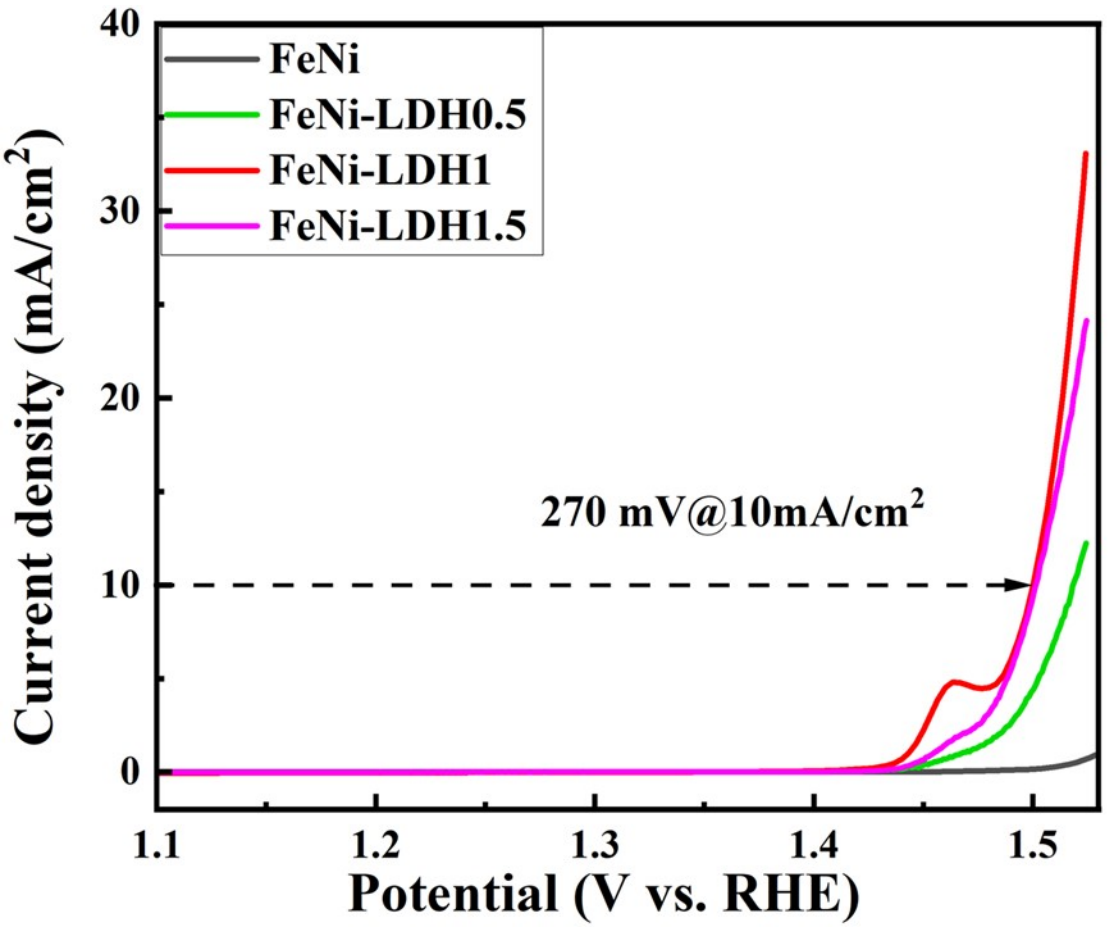

Fig. S5.IR-corrected linear sweep voltammetry (LSV) curves recorded at a scan rate of 5 mV $s^{-1}$for Fe Ni, FeNi-LDH0.5, FeNi-LDH1, and FeNi-LDH1.5 electrodes.

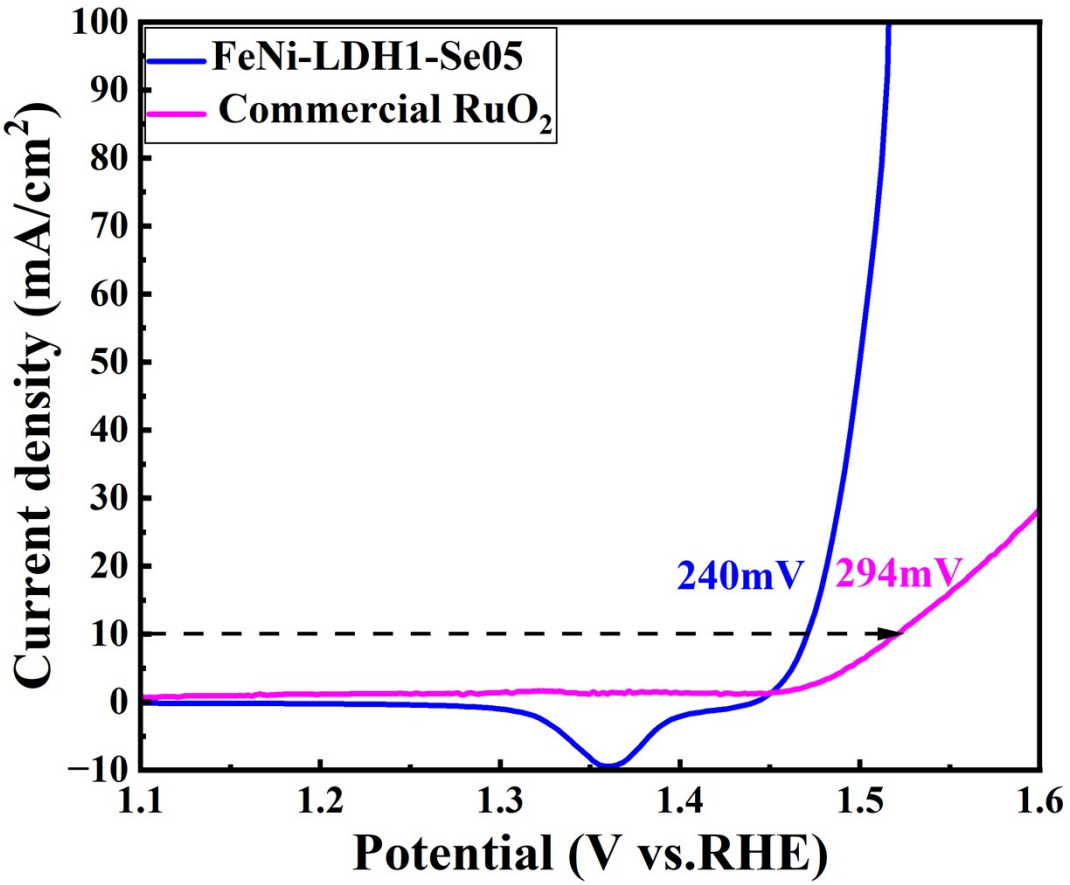

Fig. S6 .IR-corrected linear sweep voltammetry (LSV) curves recorded at a scan rate of 5 mV $s^{-1}$for FeNi-LDH05 and commercial RuO_2 electrodes.

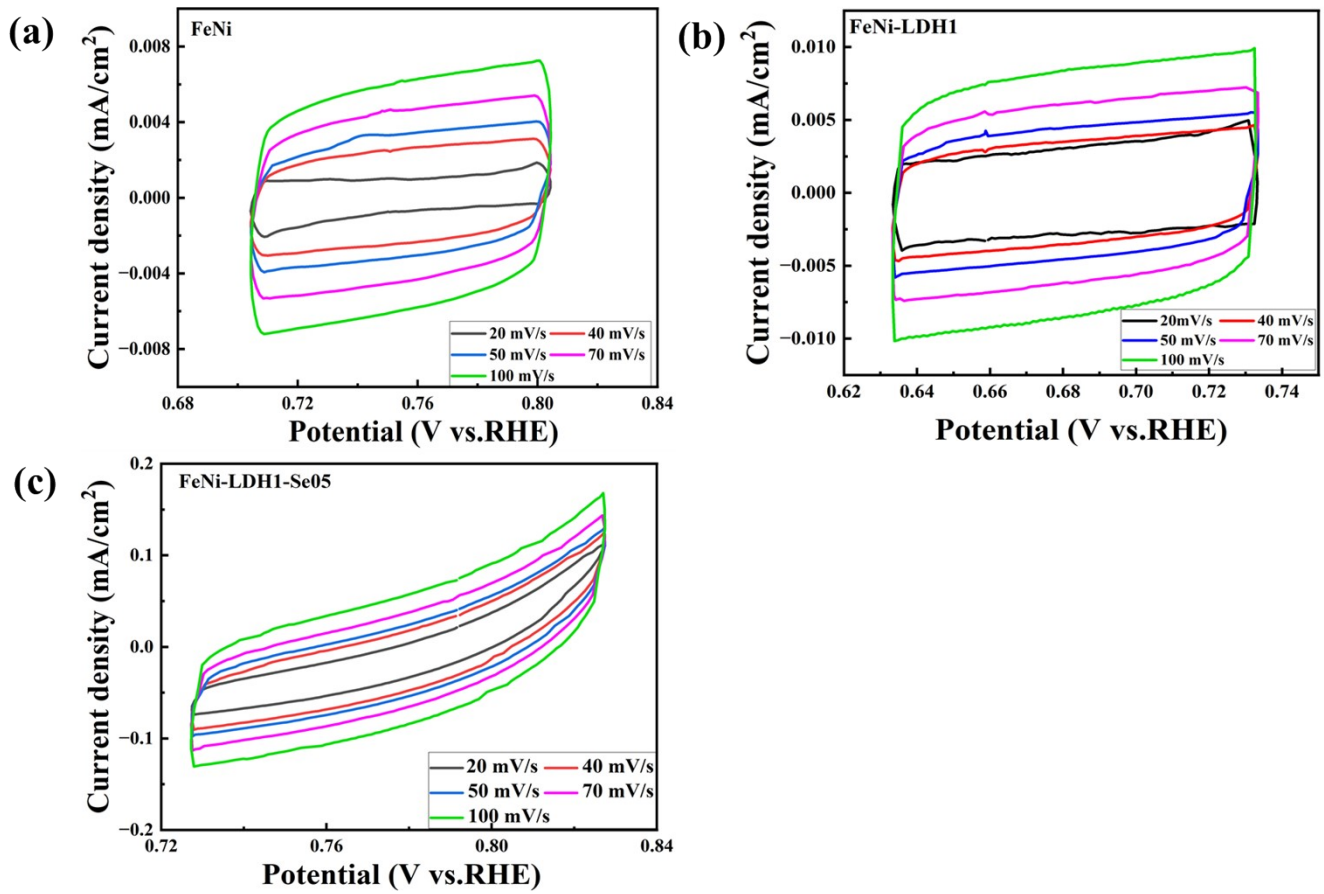

Fig. S7.CV curves at different scan rates (20, 40, 50, 70, 100) mV/s in potential window 0.1 V centered in the open circuit voltage (OCV) for (a) FeNi, (b) FeNi-LDH1, and (c) FeNi-LDH1-Se05 catalysts, respectively.

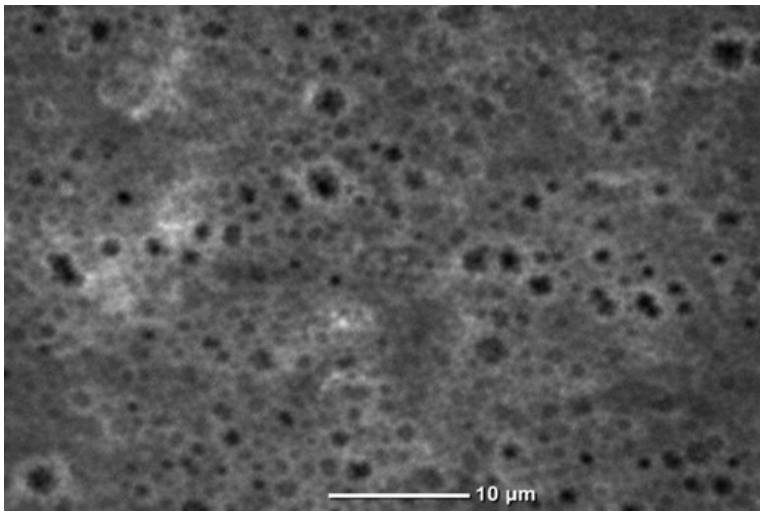

Fig. S8. SEM of the FeNi-LDH1-Se05 sample after stability at a current density of 100 mA/cm^2 for 120 hours.

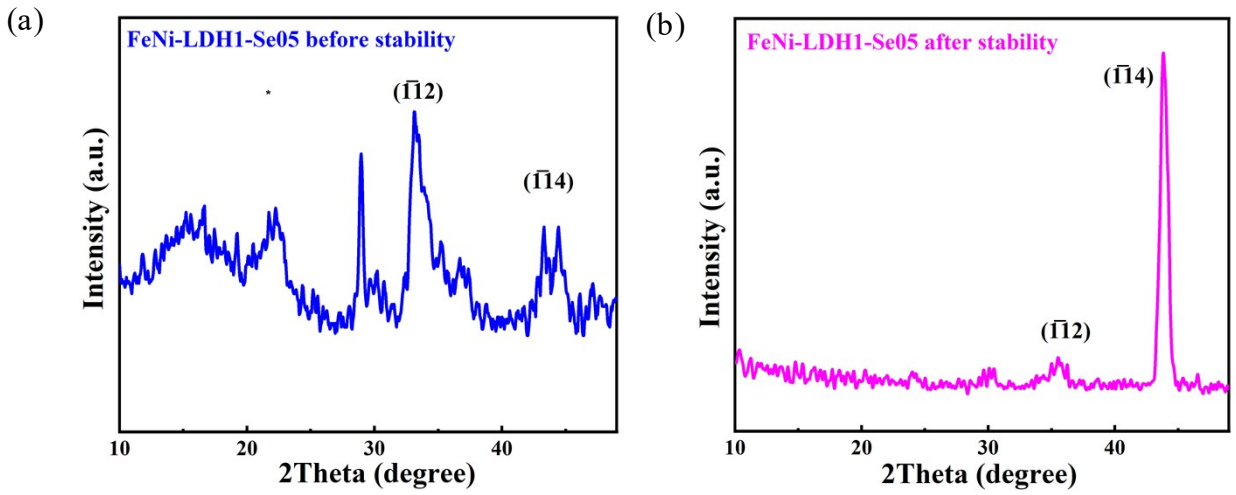

Figg. S9. Magnified XRD patterns in the 10–50° 2θ range for FeNi-LDH1-Se05 before and after stability at 100 mAcm^{-2} for 5 days.

Table 1. The comparison of OER performance of FeNi-LDH1-Se05 in 1.0 M KOH with other FeNi-based catalysts.

Catalyst	Substrate	Electrolyte	Overpotential (mV)	Tafel slope mV/dec	Stability	Ref.
FeNi-LDH1-Se0.05	Self-supporting catalyst	1.0 M KOH	240@10, 290@100 mA/cm^2	37	Excellent Stable with activity 97.4%@100mA/cm^2 for 120 h (5 days).	**This work**
Cr–FeNi LDH @ESS	SS	1.0 M KOH	280@10 mA/cm^2	44	Stable for 20 h@1.56,1.65V	1
VSe_2/NiFe-LDH	NF	1.0 M KOH	243@10, 304@100 mA/cm^2	59.5	Stable for 50h @500mA/cm^2	2
Fe OOH@NOP	NF	1.0 M KOH	336@100 mA/cm^2	69.2	Stable for 100 h@50,100mA/cm^2	3
selenized Ni Fe-LDH	GC	1 M KOH	286@10 mA/cm^2	63.6	Stable for 60h@10mA/cm^2	4
Ni Fe @Ni Cr-LDH	GC	1.0 M KOH	266@10 mA/cm^2	63	Stable for 24h@10mA/cm^2	5
Ni Fe-LDH/Ti3C2	NF	1.0 M KOH	334@10 mA/cm^2	55		6
Pt-NiFe-MOF-1.0		1.0 M KOH	253@10 mA/cm^2	62		7
Ni CoP/nickel	NF	1.0 M KOH	262@10 mA/cm^2	75	Stable for 24h@10mA/cm^2	8

foam (NF)						
(Ni_3Fe_2G/CP	CP	1.0 M KOH	300@100 mA/cm^2	74	Stable for 40h@50mA/cm^2	9
NFO/rGO	GC	1.0 M KOH	327@10 mA/cm^2	103	Stable for 8.33h@1.55 V vs. RHE	10
Ni FeP-DBD	GC	1.0 M KOH	265 @10 mA/cm^2	40.9	Stable for 20h@1.5V vs.RHE	11

Computational details

The oxygen evolution reaction, consisting of four consecutive one-electron transfer steps, was examined to enhance comprehension of the total water splitting efficiency. Every step possesses a unique Gibbs free energy alteration, which is essential for assessing the thermodynamic viability of the reaction. The four steps are:

$$H_2O(l) + * \rightarrow OH^* + H^+ + e^- \quad (1)$$

$$OH^* \rightarrow O^* + H^+ + e^- \quad (2)$$

$$H_2O(l) + O^* \rightarrow OOH^* + H^+ + e^- \quad (3)$$

$$OOH^* \rightarrow * + O_2(g) + H^+ + e^- \quad (4)$$

In this context, * signifies the catalyst's active site, (g) represents the gas phase, and *O, *OOH, and *OH identify the species adsorbed onto the catalyst's active site. The standard approach is frequently utilized in literature to calculate the reaction Gibbs free energy under typical conditions as outlined in the equations. 12 to 15.

$$\Delta G_1 = E_{HO} - E_{slab} + \frac{1}{2}E_{H_2} - E_{H_2O} + \Delta E_{ZPE} - T\Delta S \quad (5)$$

$$\Delta G_2 = E_O - E_{HO} + \frac{1}{2}E_{H_2} + \Delta E_{ZPE} - T\Delta S \quad (6)$$

$$\Delta G_3 = E_{HOO} - E_O + \frac{1}{2}E_{H_2} + \Delta E_{ZPE} - T\Delta S \quad (7)$$

$$\Delta G_4 = E_{slab} - E_{HOO} - \frac{3}{2}E_{H_2} + 2E_{H_2O} + 4.92 + \Delta E_{ZPE} - T\Delta S \quad (8)$$

where E_{HO}, E_{slab}, E_{H2}, E_{H2O}, and E_{HOO} are the energies of the OH-adsorbed and bare structures, the hydrogen molecule, the water molecule, and the HOO-adsorbed structure, respectively.

References

1 Y. Lv, X. Deng, J. Ding and Y. Zhou, *Sci. Rep.*, 2024, **14**, 902.

2 A. P. Hegde, M. P., L. S. G., A. Kumar and H. S. Nagaraja, *Int. J. Hydrog. Energy*, 2024, **71**, 1456–1467.

3 S. Hong, J. Kim, S. Kwon, K. Ham, H. Long, W. A. Goddard, K. Cho and P. J. A. Kenis, *Appl. Catal. B Environ.*, 2025, **374**, 125393.

4 Z. Wang, Y. Liang, T. Fang, X. Song, L. Yang, L. Wen, J. Wang, D. Zhao and S. Wang, *Nanomaterials*, 2025, **15**, 294. .

5 S. Liu, Y. Tang, C. Guo, Y. Liu and Z. Tang, *Materials*, 2023, **16**, 2968. .

6 Y. Sun, Z. Wang, Q. Zhou, X. Li, D. Zhao, B. Ding and S. Wang, *Heliyon*, 2024, **10**, e30966.

7 K. Zh. Bekmyrza, K. A. Kuterbekov, A. M. Kabyshev, M. M. Kubenova, A. A. Baratova, N. Aidarbekov, M. D. Chaka and N. E. Benti, *Sci. Rep.*, 2025, **15**, 28418.

8 D. Wang, Y. Zhang, T. Fei, C. Mao, Y. Song, Y. Zhou and G. Dong, *ChemElectroChem*, 2021, **8**, 3064–3072.

9 V. K. Singh, B. Malik, R. Konar, E. S. Avraham and G. D. Nessim, *Electrochem.*, 2024, **5**, 70–83.

10 P. V. Shinde, R. Samal and C. S. Rout, *Trans. Tianjin Univ.*, 2022, **28**, 80–88.

11 T. Wang, X.-Z. Fu and S. Wang, *Green Energy Environ.*, 2022, **7**, 365–371.